

## Thermodynamics, Optical Properties, and Coordination Modes of Np(V) with Dipicolinic Acid

Guoxin Tian,<sup>†</sup> Linfeng Rao,<sup>\*,†</sup> and Simon J. Teat<sup>‡</sup>

<sup>†</sup>Chemical Sciences Division, Lawrence Berkeley National Laboratory, Berkeley, California 94720, and

<sup>‡</sup>Advanced Light Source, Lawrence Berkeley National Laboratory, Berkeley, California 94720

Received June 9, 2009

Complexation of  $\text{NpO}_2^+$  with dipicolinic acid (DPA) has been investigated in 1 M  $\text{NaClO}_4$  at 25 °C. Two complexes,  $\text{NpO}_2(\text{DPA})^-$  and  $\text{NpO}_2(\text{DPA})_2^{3-}$ , were identified, and the stability constants ( $\log \beta_1$  and  $\log \beta_2$ ) were determined to be 8.68 and 12.31, respectively, by spectrophotometry. The enthalpies of the complexation ( $\Delta H_1$  and  $\Delta H_2$ ) were measured to be  $-25.2$  and  $-45.9$  kJ/mol by microcalorimetry. The entropies ( $\Delta S_1$  and  $\Delta S_2$ ) were calculated to be 81.6 and 81.8 J/(K mol) accordingly. The strong complexation of  $\text{NpO}_2^+$  with DPA is driven by both positive entropies and highly exothermic enthalpies. The crystal structure of  $\text{Na}_3\text{NpO}_2(\text{DPA})_2(\text{H}_2\text{O})_6(\text{s})$  shows that, in the  $\text{NpO}_2(\text{DPA})_2^{3-}$  complex, the Np atom sits at a center of inversion and the two DPA ligands symmetrically coordinate to Np in a tridentate mode. Due to the centrosymmetric structure of the  $\text{NpO}_2(\text{DPA})_2^{3-}$  complex, the  $f \rightarrow f$  transitions of Np(V) are forbidden, and the sharp bands originating from the  $f \rightarrow f$  transitions either disappear or become very weak in the optical absorption or diffuse reflectance spectra of the  $\text{NpO}_2(\text{DPA})_2^{3-}$  complex.

### 1. Introduction

The next-generation nuclear energy systems require the development of advanced spent nuclear fuel (SNF) reprocessing processes in which precise control of the chemical behavior of actinides and fission products is achieved. For example, by the design of the UREX+ processes currently being developed, pure uranium (U) and pure plutonium/neptunium (Pu/Np) product streams are to be obtained in the U separation step (UREX process) and the Np/Pu separation step (NPEX process), respectively.<sup>1–3</sup> However, precise control of some actinides, Np in particular, has proven difficult. Lab-scale tests indicate that 99.5% of the plutonium but only 71% of the neptunium are found in the Pu/Np product stream,<sup>2</sup> suggesting that the extractability of Np is low under

the process conditions. Probably, some of the Np in the process stream exists in its pentavalent state as  $\text{NpO}_2^+$ , and because of its low ionic charge,  $\text{NpO}_2^+$  does not form strong complexes with many ligands and is not extractable by many traditional extractants in solvent extraction. Therefore, controlling the oxidation states of Np (e.g., in a more extractable tetravalent state, Np(IV)) and searching for efficient extractants for Np(V) are of critical importance in the development of advanced SNF reprocessing processes.

Recently, amide derivatives of dicarboxylic acids have been studied as extractants for actinide separations because of their potential to make the separation processes more efficient and environmentally benign.<sup>4–10</sup> The amide ligands consist of only C, H, O, and N atoms so that they are completely incinerable. As a result, the amount of solid radioactive wastes generated in the amide-based processes could be significantly reduced. Among the ligands, amide derivatives of oxidiacetic acid (ODA)<sup>4–7</sup> and dipicolinic acid

\*Author to whom correspondence should be addressed. Tel.: 510 486 5427. Fax: 510 486 5596. E-mail: LRao@lbl.gov.

(1) Laidler, J. J.; Bresee, J. C. The Advanced Fuel Cycle Initiative of the U.S. Department of Energy: Development of Separations Technologies. In *Proceedings of WM-04 Conference*, Tucson, AZ, February 29 to March 4, 2004.

(2) Vandegrift, G. F.; Regalbuto, M. C.; Aase, S.; Arafat, H.; Bakel, A.; Bowers, D.; Byrnes, J. P.; Clark, M. A.; Emery, J. W.; Falkenberg, J. R.; Gelis, A. V.; Hafenrichter, L.; Leonard, R.; Pereira, C.; Quigley, K. J.; Tsai, Y.; Vander Pol, M. H.; Laidler, J. J. Lab-Scale Demonstration of the UREX+ Process. In *Proceedings of WM-04 Conference*, Tucson, AZ, February 29 to March 4, 2004.

(3) Vandegrift, G. F.; Regalbuto, M. C.; Aase, S.; Bakel, A.; Battisti, T. J.; Bowers, D.; Byrnes, J. P.; Clark, M. A.; Emery, J. W.; Falkenberg, J. R.; Gelis, A. V.; Pereira, C.; Hafenrichter, L.; Tsai, Y.; Quigley, K. J.; Vander Pol, M. H. Designing and Demonstration of the UREX+ Process Using Spent Nuclear Fuel. In *Proceedings of ATALANTE-2004 Conference*, Nimes, France, June 21–24, 2004.

(4) Suzuki, H.; Sasaki, Y.; Sugo, Y.; Apichaibukol, A.; Kimura, T. *Radiochim. Acta* 2004, 92, 463.

(5) Ansari, S. A.; Pathak, P. N.; Husain, M.; Prasad, A. K.; Parmar, V. S.; Manchanda, V. K. *Radiochim. Acta* 2006, 94, 307.

(6) Tian, G.; Zhang, P.; Wang, J.; Rao, L. *Solv. Extr. Ion Exch.* 2005, 23, 631.

(7) Sasaki, Y.; Choppin, G. *Radiochim. Acta* 1998, 80, 85.

(8) Babain, V. A.; Alyapyshev, M. Yu.; Kiseleva, R. N. *Radiochim. Acta* 2007, 95, 217.

(9) Lapka, J. L.; Paulenova, A.; Alyapyshev, M. Yu.; Babain, V. A.; Herbst, R. S.; Law, J. D. *Radiochim. Acta* 2009, 97, 291.

(10) Paulenova, A.; Alyapyshev, M. Yu.; Babain, V. A.; Herbst, R. S.; Law, J. D. *Sep. Sci. Technol.* 2008, 43, 2606.

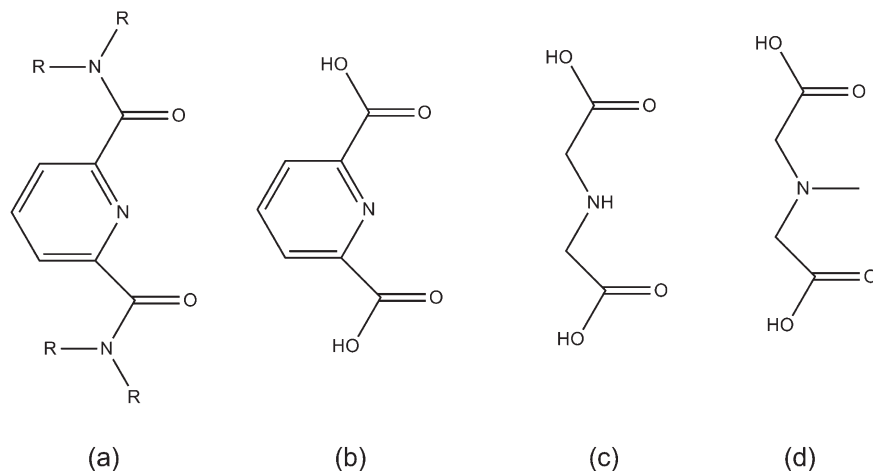


**Figure 1.** (a) Substituted dipicolinamide, R = alkyl or aryl groups; (b) dipicolinic acid (DPA); (c) iminodiacetic acid (IDA); (d) N-methyl-iminodiacetic acid (MIDA).

(DPA)<sup>8–10</sup> have been shown to be effective for extracting actinides in various oxidation states. Moderate distribution ratios were obtained for “problematic” Np(V) that is unextractable in traditional processes using tributyl phosphate as the extractant.<sup>6</sup>

To reveal the thermodynamic principle and structural factors governing the coordination of the amide derivatives of DPA with Np(V) and help to understand and improve the extraction behavior of Np(V) in SNF separation processes, we have started a systematic study of the complexation of Np(V) with a series of ligands related to DPA (Figure 1). This paper reports the thermodynamic, optical, and structural data on the complexation between Np(V) and DPA. Our previous studies on the analogous series of ODA-related ligands have shown that ODA and its amide derivatives (tetramethyl-3-oxa-glutaramide, TMOGA; dimethyl-3-oxa-glutaramic acid) all form tridentate Np(V) complexes with similar structures and that there are systematic changes in the thermodynamic driving force (enthalpy and entropy) between the carboxylic acid and the amides that could be explained by the difference in the degree of hydration.<sup>11</sup> Therefore, we expect that the thermodynamic and structural data for the complexation of Np(V) with DPA are of great relevance and high value to the understanding of the complexation of Np(V) with its amide derivatives.

Only a very limited number of thermodynamic<sup>12–14</sup> and kinetic<sup>15</sup> studies on the complexation of NpO<sub>2</sub><sup>+</sup> with DPA have been reported in the literature. As to the thermodynamic data, only a few stability constants of the 1:1 Np(V)–DPA complex were determined with solvent extraction,<sup>12</sup> spectrophotometry, and potentiometry,<sup>13</sup> and the values differ by a few orders of magnitude (log β<sub>1</sub> ranging from 4.12 to 8.19). There has been only one study that measured the enthalpy of the 1:1 complexation by calorimetry.<sup>14</sup> In none of the previous studies was the 1:2 Np(V)–DPA complex identified,

which is surprising because DPA seems to be a fairly strong ligand and the equatorial plane of NpO<sub>2</sub><sup>+</sup> should be able to accommodate two such tridentate ligands. In fact, in the analogous ODA and TMOGA systems, 1:2 Np(V) complexes have been identified by thermodynamic measurements and X-ray crystallography.<sup>16,17</sup> In addition, a 1:2 Np(V)–DPA complex in the [Li<sub>3</sub>NpO<sub>2</sub>(DPA)(H<sub>2</sub>O)<sub>6</sub>] crystal has been reported.<sup>18</sup> We hypothesize that a 1:2 Np(V)–DPA complex also forms in solution but might have been “missed” in previous studies either because insufficient ligand concentrations were used or because this complex may possess an inversion center, as in the Np(V)–ODA<sup>16</sup> and Np(V)–TMOGA<sup>17</sup> complexes, so that it is “silent” in optical absorption. The objectives of this study are three-fold: (1) to test the above hypothesis and characterize the structure of the 1:2 Np(V)–DPA complex, (2) for the first time, to determine the thermodynamic parameters (stability constants, enthalpy, and entropy) for the 1:2 Np(V)–DPA complex, and (3) to re-evaluate the stability constant of the 1:1 Np(V)–DPA complex and reconcile the discrepancy in the literature.

It is noted that, in contrast to a large number of structures of UO<sub>2</sub><sup>2+</sup>–DPA complexes,<sup>19–29</sup> only two structures of

(11) Tian, G.; Rao, L.; Teat, S. J.; Liu, G. *Chem. Eur. J.* **2009**, *15*, 4172.  
 (12) Inoue, Y.; Tochiyama, O. *Polyhedron* **1983**, *2*, 627.  
 (13) Rizkalla, E. N.; Nectoux, F.; Dabos-Seignon, S.; Pages, M. *Radiochim. Acta* **1990**, *51*, 151.  
 (14) Choppin, G. R.; Rao, L. F.; Rizkalla, E. N.; Sullivan, J. C. *Radiochim. Acta* **1992**, *57*, 173.  
 (15) Friese, J. I.; Nash, K. L.; Jensen, M. P.; Sullivan, J. C. *Radiochim. Acta* **2001**, *89*, 35.

(16) Tian, G.; Rao, L.; Oliver, A. *Chem. Commun.* **2007**, 4119.  
 (17) Tian, G.; Xu, J.; Rao, L. *Angew. Chem., Int. Ed.* **2005**, *44*, 6200.  
 (18) Andreev, G. B.; Antipin, M. Yu.; Fedoseev, A. M.; Budantseva, N. A. *Dokl. Chem.* **2000**, *374*, 187.  
 (19) Brayshaw, P. A.; Hall, A. K.; Harrison, W. T. A.; Harrowfield, J. M.; Pearce, D.; Shand, T. M.; Skelton, B. W.; Whitaker, C. R.; White, A. H. *Eur. J. Inorg. Chem.* **2005**, 1127 and references cited therein.  
 (20) Ghosh, S. K.; Bharadwaj, P. K. *Inorg. Chem.* **2003**, *42*, 8250. (b) Ghosh, S. K.; Bharadwaj, P. K. *Inorg. Chem.* **2004**, *43*, 2293.  
 (21) Jain, S. L.; Slawin, A. M. Z.; Woollins, J. D.; Bhattacharyya, P. *Eur. J. Inorg. Chem.* **2005**, 721.  
 (22) Gonzalez-Baró, A. C.; Castellano, E. E.; Piro, O. E.; Parajón-Costa, B. S. *Polyhedron* **2005**, *24*, 49.  
 (23) Goher, M. A. S.; Mautner, F. A.; Hafez, A. K.; Youssef, A. A. *Polyhedron* **2003**, *22*, 515 and references cited therein.  
 (24) Immirzi, A.; Bombieri, G.; Degetto, S.; Marangoni, G. *Acta Crystallogr., Sect. B* **1975**, *31*, 1023.  
 (25) Masci, B.; Thuéry, P. *Polyhedron* **2005**, *24*, 229.  
 (26) Cousson, A.; Nectoux, F.; Pagès, M.; Rizkalla, E. N. *Radiochim. Acta* **1993**, *61*, 177.  
 (27) Frisch, M.; Cahill, C. L. *Dalton Trans.* **2006**, 4679.  
 (28) Cousson, A.; Proust, J.; Rizkalla, E. N. *Acta Crystallogr., Sect. C* **1991**, *47*, 2065.  
 (29) Harrowfield, J. M.; Lugan, N.; Shahverdizadeh, G. H.; Souidi, A. A.; Thuéry, P. *Eur. J. Inorg. Chem.* **2006**, 389.

$\text{NpO}_2^+$ –DPA complexes have been reported,  $[\text{Li}_3\text{NpO}_2\text{-(DPA)(H}_2\text{O)}_6]$  (space group  $P21/n$ )<sup>18</sup> and  $[(\text{NpO}_2)_2(\text{DPA})(\text{H}_2\text{O})_5]$  (space group  $C2/c$ ).<sup>30</sup> No inversion centers exist in either of the two structures.

## 2. Experimental Section

**2.1. Chemicals.** All chemicals were reagent-grade or higher. Boiled Milli-Q water was used in preparation of all of the solutions. All experiments were conducted at 25 °C and an ionic strength of 1.0 M ( $\text{NaClO}_4$ ). The stock solution of  $\text{Np(V)}$  in perchloric acid was prepared as described elsewhere.<sup>31</sup> The concentration of  $\text{Np(V)}$  was determined by the absorbance at 980.2 nm ( $\epsilon = 395 \text{ M}^{-1} \text{ cm}^{-1}$ ), and the concentration of perchloric acid in the stock solution was determined by Gran's titration.<sup>32</sup> Dipicolinic acid (or pyridine-2,6-dicarboxylic acid, DPA, 98%) from Avocado Research Chemicals Ltd. was used as received. Buffered DPA solutions were prepared by neutralizing weighted DPA with a standard  $\text{NaOH}$  solution ( $0.99900 \pm 0.00196 \text{ M}$ , Brinkmann) and diluting it to appropriate concentrations.

**2.2. Spectrophotometry.** Spectrophotometric titrations of  $\text{NpO}_2^+$  were carried out on a Cary 6000i spectrophotometer (Varian Inc.) from 1150 to 950 nm with an interval of 0.1 nm. A total of 2.5 mL of the  $\text{NpO}_2^+$  solution was put in a 1 cm cuvette, into which appropriate aliquots of buffered DPA solutions were added and mixed thoroughly (for 1–2 min) before the spectrum was collected. Preliminary kinetic experiments showed that the complexation reaction was fast, and the absorbance became stable within 30 s of mixing. Usually, 15–20 additions were made, generating a set of 16–21 spectra in each titration. Multiple titrations with different concentrations of  $\text{Np(V)}$  were performed. The formation constants were calculated by the nonlinear regression program Hyperquad 2000.<sup>33</sup>

Diffuse reflectance spectra of solid samples were collected from 1150 to 400 nm with an interval of 0.1 nm and a fixed spectral bandwidth of 0.5 nm with the diffuse reflectance accessory of the Cary 6000i, DRA-1800. The sample was prepared by placing 2 mg of the solid compound between two  $1 \times 1$  in. quartz plates and sealing it with tape. A piece of white filter paper was taped on one side of the sample unit as the background, while the other side was open to the light beam.

**2.3. Microcalorimetry.** Calorimetric titrations were conducted at 25 °C with an isothermal microcalorimeter (Model ITC 4200, Calorimetry Sciences Corp.). Procedures and results of the calibration of the calorimeter were provided elsewhere.<sup>34</sup> Three titrations with different concentrations of  $\text{NpO}_2^+$  (1.0–2.5 mM) were performed to reduce the uncertainty of the results. In all titrations, 0.9 mL of  $\text{NpO}_2^+$  solution was put in the reaction cell, and  $n$  additions of 0.005 mL of the titrant were made ( $n = 40\text{--}50$ ) through a 0.250 mL syringe, resulting in  $n$  experimental values of total heat ( $Q_{\text{ex},j}$ ,  $j = 1\text{--}n$ ). These values were corrected for the heats of titrant dilution ( $Q_{\text{dil},j}$ ) that were measured in a separate run. The net reaction heat at the  $j$ th point ( $Q_{\text{r},j}$ ) was obtained from the difference:  $Q_{\text{r},j} = Q_{\text{ex},j} - Q_{\text{dil},j}$ . The value of  $Q_{\text{r},j}$  is a function of the concentrations of the reactants ( $C_{\text{Np}}$ ,  $C_{\text{H}}$ , and  $C_{\text{DPA}}$ ), the equilibrium constants, and the enthalpies of the reactions that occurred in the titration. A least-squares minimization program, Letagrop,<sup>35</sup> was

**Table 1.** Crystal Data and Structure Refinement for  $\text{Na}_3\text{NpO}_2(\text{DPA})_2(\text{H}_2\text{O})_6$

chemical formula	$\text{C}_{14}\text{H}_{18}\text{N}_2\text{Na}_3\text{NpO}_{16}$
fw	776.27
temperature	150(2) K
radiation, wavelength	synchrotron, 0.77490 Å
crystal system, space group	triclinic, $P\bar{1}$
unit cell parameters	$a = 6.7731(4) \text{ Å}$ , $\alpha = 70.547(2)^\circ$ $b = 8.6970(6) \text{ Å}$ , $\beta = 74.312(2)^\circ$ $c = 10.4826(7) \text{ Å}$ , $\gamma = 69.755(2)^\circ$
cell volume	$537.80(6) \text{ Å}^3$
Z	1
calculated density	$2.397 \text{ g/cm}^3$
abs coeff $\mu$	$4.227 \text{ mm}^{-1}$
F(000)	370
cryst color, size	colorless, $0.07 \times 0.03 \times 0.02 \text{ mm}^3$
reflns for cell refinement	5617 ( $\theta$ range $3.05$ to $33.58^\circ$ )
data collection method	Bruker APEX II CCD diffractometer $\omega$ rotation with narrow frames
$\theta$ range for data collection	$2.82$ to $33.71^\circ$
index ranges	$h = -9$ to $+9$ , $k = -12$ to $+12$ , $l = -14$ to $+15$
completeness to $\theta = 30.00^\circ$	98.6%
reflns collected	7579
independent reflns	3214 ( $R_{\text{int}} = 0.0563$ )
reflns with $F^2 > 2\sigma$	3214
abs correction	semiempirical from equivalents
min. and max. transmission	0.69 and 0.85
structure solution	direct methods
refinement method	full-matrix least-squares on $F^2$
weighting params $a, b$	0.0809, 3.8918
data/restraints/params	3214/6/166
final R indices [ $F^2 > 2\sigma$ ]	$R1 = 0.0461$ , $wR2 = 0.1353$
R indices (all data)	$R1 = 0.0461$ , $wR2 = 0.1353$
goodness-of-fit on $F^2$	1.088
largest and mean shift/su	0.001 and 0.000
largest diff. peak and hole	1.746 and $-1.666 \text{ e Å}^{-3}$

used to calculate the enthalpy of complexation of  $\text{NpO}_2^+$  with DPA.

**2.4. Single-Crystal X-Ray Diffractometry.** Colorless crystals of the 1:2  $\text{Np(V)}$ –DPA complex,  $\text{Na}_3\text{NpO}_2(\text{DPA})_2(\text{H}_2\text{O})_6$ , were obtained by slow evaporation from 0.1 mL of a 0.05 M  $\text{NpO}_2(\text{ClO}_4)$  solution containing 0.1 M DPA at pH 6–7. Representative crystals were sealed in glass capillary tubes and mounted on the goniometer. Diffraction data were collected on a Bruker APEXII diffractometer at Beamline 11.3.1 of the Advanced Light Source, Lawrence Berkeley National Laboratory. Details of the crystallographic data are provided in Table 1.

## 3. Results

**3.1. Identification of  $\text{Np(V)}$ –DPA Complexes in Solution.** Figure 2 shows a representative set of absorption spectra in the near IR region for the titration of  $\text{NpO}_2^+$  with DPA. The changes in the spectra of  $\text{Np(V)}$  can be discussed in phase I and phase II, as shown in Figure 2a and b, respectively. In phase I ( $C_{\text{DPA}}/C_{\text{Np}} = 0\text{--}1$ ), as the DPA solution was added, the intensities of the absorption bands at 980, 1024, 1097, and 1117 nm that belong to the free  $\text{NpO}_2^+$  decreased, while new corresponding bands appeared at longer wavelengths (990, 1045, 1103, and 1138 nm), indicating the formation of a new  $\text{Np(V)}$  species. The new bands were assigned to the  $\text{NpO}_2(\text{DPA})^-$  complex because a Job plot<sup>36</sup> (absorbance versus  $C_{\text{DPA}}/C_{\text{Np}}$ ) suggested a 1:1  $\text{Np(V)}$ /DPA stoichiometry, and because the band positions agree with those of the 1:1 complex previously observed.<sup>13,14</sup> In phase II ( $C_{\text{DPA}}/C_{\text{Np}} > 1$ ), as

(30) Andreev, G. B.; Khrestalev, V. N.; Antipin, M. Y.; Fedoseev, A. M.; Budantseva, N. A.; Krupa, Z. K.; Madic, C. *Russ. J. Coord. Chem.* **2000**, *26*, 825.

(31) Rao, L.; Srinivasan, T. G.; Garnov, A. Yu.; Zanonato, P.; Di Bernardo, P.; Bismundo, A. *Geochim. Cosmochim. Acta* **2004**, *68*, 4821.

(32) Gran, G. *Analyst* **1952**, *77*, 661.

(33) Gans, P.; Sabatini, A.; Vacca, A. *Talanta* **1996**, *43*, 1739.

(34) Zanonato, P.; Di Bernardo, P.; Bismundo, A.; Liu, G.; Chen, X.; Rao, L. *J. Am. Chem. Soc.* **2004**, *126*, 5515.

(35) Arnek, R. *Ark. Kemi* **1970**, *32*, 81.

(36) Job, P. *Ann. Chim. (Paris)* **1928**, *9*, 113.

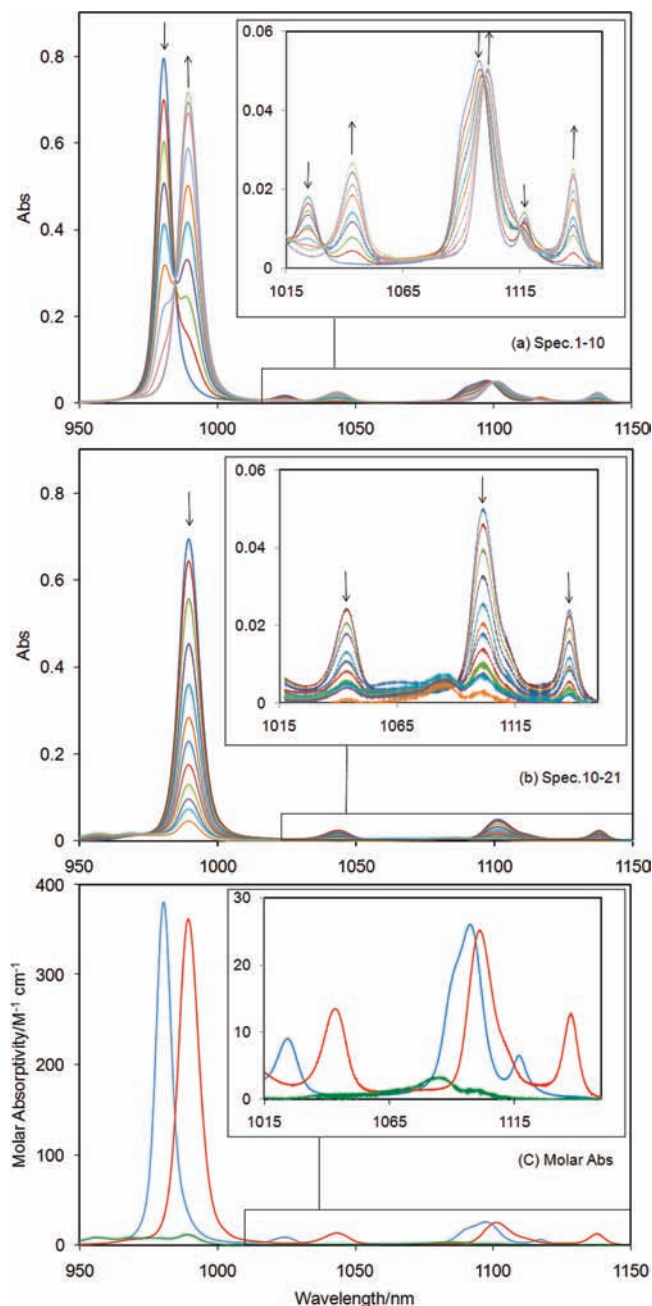


**Figure 2.** Spectrophotometric titrations of  $\text{NpO}_2^+$  with DPA ( $t = 25^\circ\text{C}$ ,  $I = 1.0\text{ M NaClO}_4$ ). Initial solution:  $V^0 = 2.50\text{ mL}$ ,  $C_{\text{Np}}^0 = 2.01\text{ mM}$ ,  $C_{\text{H}}^0 = 1.72\text{ mM}$ . Titrant:  $0.025\text{ M Na}_2\text{DPA}$ , a total of  $1.575\text{ mL}$  added. Optical path =  $1.0\text{ cm}$ . The 21 spectra shown are normalized in terms of  $C_{\text{Np}}^0$ . (a) Phase I ( $C_{\text{DPA}}/C_{\text{Np}} = 0-1$ ), spectra nos. 1–10. (b) Phase II ( $C_{\text{DPA}}/C_{\text{Np}} > 1$ ), spectra nos. 10–21. (c) Deconvoluted spectra of  $\text{NpO}_2^+$  (blue),  $\text{NpO}_2(\text{DPA})^-$  (red), and  $\text{NpO}_2(\text{DPA})_2^{3-}$  (green).

the concentration of DPA was further increased, the intensities of these bands gradually decreased, but no new absorption bands appeared (Figure 2b). With a sufficiently high concentration of DPA, the spectra could become flat and featureless. The variation of spectra in Figure 2 is very similar to those observed in the complexations of  $\text{NpO}_2^+$  with ODA<sup>16</sup> and TMOGA<sup>17</sup> and can be interpreted with the same hypothesis previously discussed; that is, two complexes of  $\text{NpO}_2^+$  with DPA formed successively during the titration, but the second complex,  $\text{NpO}_2(\text{DPA})_2^{3-}$ , did not absorb in the

wavelength region. Factor analysis by Hyperquad 2000 confirmed that there were only two absorbing species (free  $\text{NpO}_2^+$  and the first  $\text{Np}(\text{V})$ –DPA complex) in the solution, supporting this hypothesis. Therefore, the spectrophotometric data were fitted with the formation of  $\text{NpO}_2(\text{DPA})^-$  and  $\text{NpO}_2(\text{DPA})_2^{3-}$ . Deconvoluted spectra were also obtained by using Hyperquad 2000. As shown in Figure 2c, the spectrum of  $\text{NpO}_2(\text{DPA})^-$  has all absorption bands (990, 1045, 1103, 1138 nm) that correspond to those of free  $\text{NpO}_2^+$  (980, 1024, 1097, 1117 nm), but they are red-shifted. In contrast, the spectrum of  $\text{NpO}_2(\text{DPA})_2^{3-}$  is almost flat and featureless, indicating that  $\text{NpO}_2(\text{DPA})_2^{3-}$  does not absorb the light in this wavelength region.

The stability constants ( $\log \beta$ ) of  $\text{NpO}_2(\text{DPA})^-$  and  $\text{NpO}_2(\text{DPA})_2^{3-}$  were calculated to be  $(8.68 \pm 0.11)$  and  $(12.31 \pm 0.11)$ , respectively ( $I = 1.0\text{ M NaClO}_4$  and  $t = 25^\circ\text{C}$ ). In Table 2, the value of  $\log \beta_1$  from this work is compared with those from previous studies. The value of  $\log \beta_2$  from this work is the only value available for  $\text{NpO}_2(\text{DPA})_2^{3-}$ , because this complex has not been identified in previous studies.

**3.2. Enthalpy of Complexation.** Figure 3 shows a representative calorimetric titration of  $\text{Np}(\text{V})$ –DPA complexation. The total reaction heat,  $Q_{r,i}$ , as well as the distribution of  $\text{Np}(\text{V})$  species, is shown as a function of the titrant volume. From the reaction heat and the stability constants of the  $\text{Np}(\text{V})$ –DPA complexes, the enthalpies of complexation for the 1:1 and 1:2  $\text{Np}(\text{V})$ –DPA complexes were calculated to be  $-(25.2 \pm 0.7)$  and  $-(45.9 \pm 1.4)\text{ kJ/mol}$ , respectively. The entropies of complexation for the 1:1 and 1:2  $\text{Np}(\text{V})$ –DPA complexes are accordingly calculated and listed in Table 2.

**3.3. Crystal Structure of  $\text{Na}_3\text{NpO}_2(\text{DPA})_2(\text{H}_2\text{O})_6$ .** The sodium salt of the 1:2  $\text{Np}(\text{V})$ –DPA complex,  $\text{Na}_3\text{NpO}_2(\text{DPA})_2(\text{H}_2\text{O})_6$ , crystallized in a triclinic space group,  $P\bar{1}$ . The structure is shown in Figure 4, and selected bond lengths ( $\text{\AA}$ ) and bond angles (deg) are provided in Table 3. In the unit cell, the Np atom is located at an inversion center at  $[0, 0, -1]$ . The Na atoms are not shown in Figure 4, but one Na atom also lies at an inversion center at  $[0, -0.5, -0.5]$ . The axial  $\text{O}=\text{Np}=\text{O}$  moiety is perfectly linear ( $180^\circ$  angle) and symmetrical (two  $\text{Np}=\text{O}$  bonds are equal in length,  $1.825(6)\text{ \AA}$ ). The  $\text{O}=\text{Np}=\text{O}$  moiety is coordinated equatorially by two DPA ligands (Figure 4). Each DPA ligand is tridentate and coordinates to Np with the N atom of the pyridine and two O atoms of two different carboxylate groups. The bond lengths between Np and the two carboxylate oxygens are slightly different ( $R_{\text{Np}-\text{O}3} = 2.563(5)\text{ \AA}$  and  $R_{\text{Np}-\text{O}4} = 2.562(6)\text{ \AA}$ ), and one oxygen (O4) is slightly aberrant away from the coplane of the two DPA ligands. The symmetry of the  $\text{NpO}_2(\text{DPA})_2^{3-}$  unit is very similar to that of the  $\text{NpO}_2(\text{ODA})_2^{3-}$  unit in  $\text{Na}_3\text{NpO}_2(\text{ODA})_2(\text{H}_2\text{O})_2$ ,<sup>16</sup> but lower than that of  $\text{NpO}_2(\text{TMOGA})_2^+$  in  $\text{NpO}_2(\text{TMOGA})_2\text{ClO}_4$  where Np(V) is located at the cross point of three mirror planes perpendicular to each other.<sup>17</sup> Nevertheless, in all three complexes, the Np atom is at an inversion center.

The structure of  $\text{Na}_3\text{NpO}_2(\text{DPA})_2(\text{H}_2\text{O})_6$  from this work is very different from the structure of previously identified  $\text{Li}_3\text{NpO}_2(\text{DPA})_2(\text{H}_2\text{O})_6$ .<sup>18</sup> In the latter, the coordination modes of the two DPA units are not

**Table 2.** Thermodynamic Parameters of the Complexation of  $\text{NpO}_2^{+}$  with DPA and Other Ligands ( $t = 25\text{ }^\circ\text{C}$ )<sup>a</sup>

reaction	ligand	$I, \text{M}$	method	$\log \beta$	$\Delta H, \text{kJ/mol}$	$\Delta S, \text{J/(K mol)}$	ref
$\text{NpO}_2^{+} + \text{L}^{2-} = \text{NpO}_2\text{L}^{-}$	DPA	1.0	sp, cal	$8.68 \pm 0.11$	$-25.2 \pm 0.7$	$81.6 \pm 2.5$	p.w.
		0.5	sp, cal	8.19	-31.6	51.0	14
		1.0	sx	7.07, 7.25			12
		0.5	sp, pot	4.82			13
	IDA	1.0	sp, pot	5.88	-16.0	59.0	37
		0.5	sp, pot	5.81			13
		0.1	ix	6.27			38
MIDA	0.1	ix	7.37			38	
	1.0		7.0			b	
	1.0	sp, cal,	$12.31 \pm 0.11$	$-45.9 \pm 1.4$	$81.8 \pm 5.5$	p.w.	

<sup>a</sup> Ligands: DPA, dipicolinic acid; IDA, iminodiacetic acid; MIDA, N-methyl-iminodiacetic acid. Legends: sp, spectrophotometry; cal, calorimetry; pot, potentiometry; sx, solvent extraction; ix, ion exchange; p.w., present work. <sup>b</sup> Value estimated for MIDA in this work, based on the difference of  $\log \beta$  ( $\text{NpO}_2(\text{IDA})^{-}$ ) at  $I = 0.1 \text{ M}$  and that at  $1.0 \text{ M}$  and the generalization that the values of  $\log \beta$  for metal-carboxylate complexes at  $1.0 \text{ M}$  are usually  $0.3\text{--}0.4$  units lower than those at  $0.1 \text{ M}$ .<sup>39</sup>

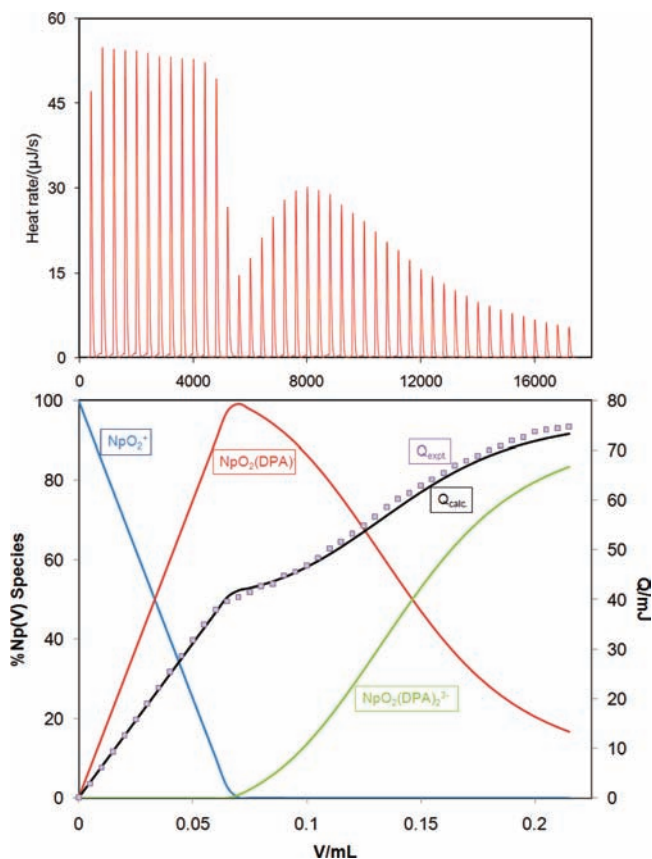


**Figure 3.** Calorimetric titration of the complexation of  $\text{Np(V)}$ –DPA ( $t = 25\text{ }^\circ\text{C}$ ,  $I = 1.0 \text{ M NaClO}_4$ ). Initial cup solution:  $V^0 = 0.900 \text{ mL}$ ,  $C_{\text{H}} = 1.15 \text{ mM}$ ,  $C_{\text{Np}} = 1.86 \text{ mM}$ . Titrant:  $C_{\text{Na}_2\text{DPA}} = 0.025 \text{ M}$ , a total of 43 additions ( $0.005 \text{ mL}$  each). Top, thermogram (the title of  $x$  axis: time/s); bottom, total heat (right  $y$  axis; open symbol, experimental; line, calculated) and speciation of  $\text{Np(V)}$  (left  $y$  axis, lines) versus the volume of the titrant.

identical ( $\mu_5^-$  and  $\mu_4^-$ , respectively), and no center of inversion exists. The difference in the cationic radii between  $\text{Na}^+$  and  $\text{Li}^+$  could be one of the reasons for the difference in the structure of the two crystals.

**3.4. Diffuse Reflectance Spectra.** The diffuse reflectance spectrum of solid  $\text{Na}_3\text{NpO}_2(\text{DPA})_2(\text{H}_2\text{O})_6$  is shown in Figure 5, in comparison with that of solid  $\text{NpO}_2\text{ClO}_4 \cdot (\text{H}_2\text{O})_x$  and the absorption spectrum of  $\text{NpO}_2^{+}$  in solution. Sharp peaks that are typical of  $f \rightarrow f$  transitions are intense in the latter two spectra but very weak in the

diffuse reflectance spectrum of solid  $\text{Na}_3\text{NpO}_2(\text{DPA})_2(\text{H}_2\text{O})_6$ .

## 4. Discussion

**4.1. Thermodynamic Trends. Reconciliation of the Difference in  $\log \beta_1$  for  $\text{NpO}_2(\text{DPA})^{-}$  from Different Studies.** The values of  $\log \beta_1$  in the literature range from 4.82 to 8.19 at  $I = 0.1$  to  $1.0 \text{ M}$  (Table 2). The value from this work ( $8.68$  at  $I = 1.0 \text{ M}$ ) is in fairly good agreement with one previous value ( $8.19$  at  $I = 0.5 \text{ M}$ ) obtained by spectrophotometry using a competing cation,<sup>14</sup> given the difference in the ionic strength and the technique (the accuracy of stability constants determined by a competition method depends on the accuracy of the known stability constants of the competing cation complex). In contrast, the value of  $4.82$  for  $\log \beta_1$  at  $I = 0.5 \text{ M}$ <sup>13</sup> is much lower and is believed to be erroneous, probably due to the negligence of the formation of the second  $\text{Np(V)}$ –DPA complex. As shown by this work, the  $\text{NpO}_2(\text{DPA})_2^{3-}$  complex is spectroscopically “silent” in the near-IR region, and failure to include it in the analysis of the spectrophotometric data would result in error. In fact, problems with spectra convergence in the data processing were noted in previous studies.<sup>13,14</sup> The values of  $\log \beta_1$  obtained by solvent extraction ( $7.07$  and  $7.25$  at  $I = 1.0 \text{ M}$ )<sup>12</sup> are also lower than that obtained in this work. We do not have a satisfactory explanation for this discrepancy but would like to point out that cautions should be taken when comparing results from drastically different techniques. It is noted that the data obtained by solvent extraction seem to be sensitive to the choice of the extractant concentration and the diluent. Using different concentrations of the extractant (TTA and phenanthroline) and diluent resulted in values of  $\log \beta_1$  that differed by  $0.2$  units.<sup>12</sup>

**Stability Constants of  $\text{Np(V)}$  Complexes with Three Structurally Related Ligands:  $\text{NpO}_2(\text{DPA})^{-}$ ,  $\text{NpO}_2(\text{IDA})^{-}$ , and  $\text{NpO}_2(\text{MIDA})^{-}$ .** Data in Table 2 indicate that  $\text{Np(V)}$  forms a much stronger 1:1 complex with DPA than iminodiacetic acid (IDA) or N-methyliminodiacetic acid (MIDA) (see the structure schematics in Figure 1):  $\text{NpO}_2(\text{DPA})^{-} > \text{NpO}_2(\text{MIDA})^{-} > \text{NpO}_2(\text{IDA})^{-}$ . The observation that MIDA forms a stronger  $\text{Np(V)}$  complex than IDA could be rationalized by the difference in the basicity of the two ligands—the  $\text{pK}_a$  of HL is  $9.59$  for MIDA and

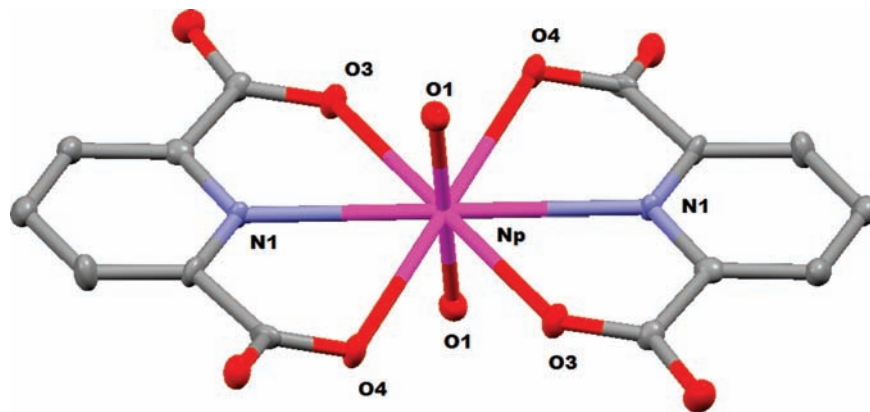


**Figure 4.** Structure of the  $\text{NpO}_2(\text{DPA})_2^{3-}$  complex in the single crystal of  $\text{Na}_3\text{NpO}_2(\text{DPA})_2(\text{H}_2\text{O})_6$  (50% probability ellipsoids). The H and Na atoms and water molecules are not shown for clarity. Np, purple; O, red; C, gray; and N, blue.

**Table 3.** Selected Bond Lengths (Å) and Bond Angles (deg) in  $\text{Na}_3\text{NpO}_2(\text{DPA})_2(\text{H}_2\text{O})_6$

Np(1)–O(1)	1.825(6)	Np(1)–O(1A)	1.825(6)
Np(1)–O(3)	2.563(5)	Np(1)–O(3A)	2.563(5)
Np(1)–N(1)	2.671(6)	Np(1)–N(1A)	2.671(6)
Np(1)–O(4)	2.562(6)	Np(1)–O(4A)	2.562(6)
O(1)–Np(1)–O(1A)	180.000(1)	O(1)–Np(1)–O(3)	93.2(2)
O(1A)–Np(1)–O(3A)	93.2(2)	O(1)–Np(1)–O(3A)	86.8(2)
O(1A)–Np(1)–O(3)	86.8(2)	O(1)–Np(1)–N(1)	84.2(2)
O(1A)–Np(1)–N(1)	95.8(2)	O(1A)–Np(1)–N(1A)	84.2(2)
O(1)–Np(1)–N(1A)	95.8(2)	O(1)–Np(1)–O(4)	91.9(2)
O(1A)–Np(1)–O(4A)	91.9(2)	O(1)–Np(1)–O(4A)	88.1(2)
O(1A)–Np(1)–O(4)	88.1(2)	O(3)–Np(1)–O(3A)	179.999(1)
O(3)–Np(1)–N(1)	59.61(18)	O(3A)–Np(1)–N(1)	120.39(18)
O(3A)–Np(1)–N(1A)	59.61(18)	O(3)–Np(1)–N(1A)	120.39(18)
O(3)–Np(1)–O(4)	118.39(17)	O(3A)–Np(1)–O(4A)	118.39(17)
O(3A)–Np(1)–O(4)	61.62(17)	O(3)–Np(1)–O(4A)	61.61(17)
N(1)–Np(1)–N(1A)	179.999(1)	N(1)–Np(1)–O(4)	59.98(17)
N(1)–Np(1)–O(4A)	120.02(17)	N(1A)–Np(1)–O(4A)	59.98(17)

9.34 for IDA at 25 °C and 0.1 M ionic strength.<sup>39</sup> The electron-donating methyl group makes the nitrogen as well as the carboxylate group of MIDA more basic than those of IDA, resulting in stronger complexation of Np(V) with the former. However, the same rationalization cannot explain why DPA forms a much stronger complex with Np(V) than IDA or MIDA, since the  $\text{p}K_a$  of DPA is only 4.7 under similar conditions.<sup>39</sup> We believe that the strong binding ability of DPA probably results from its “rigid” and conjugated structure in which the pyridine nitrogen and two carboxylate oxygen atoms are arranged at optimal positions to coordinate with  $\text{NpO}_2^+$  through its equatorial plane. As shown in Table 3, the  $\angle\text{O}–\text{Np}–\text{N}$  angles are all very close to  $60^\circ$ , and the six donor atoms (four O and two N) coordinate with Np, forming four five-membered rings in a nearly perfect hexagonal structure. The rigid structure of DPA helps to reduce the preorganization energy that is otherwise required in the complexation of Np(V) with more flexible ligands such as IDA or MIDA.

**The Newly Identified  $\text{NpO}_2(\text{DPA})_2^{3-}$  Complex.** This complex was first identified in this work, and there are no stability constants in the literature for comparison. As

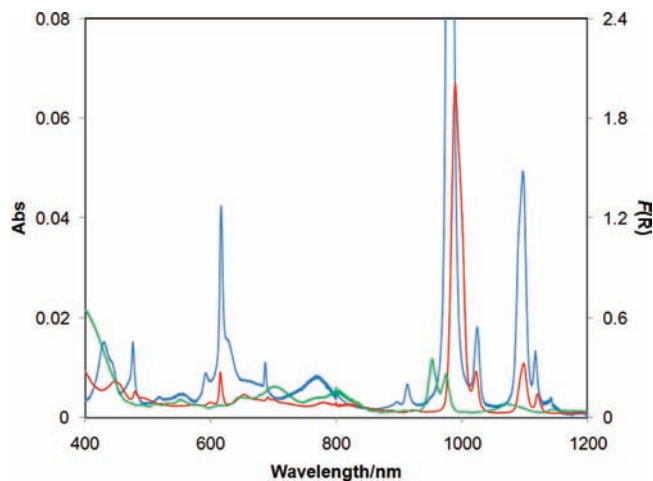


**Figure 5.** Diffuse reflectance spectra (right y axis) of  $\text{Na}_3\text{NpO}_2(\text{DPA})_2(\text{H}_2\text{O})_6$  (s) (green) and  $\text{NpO}_2\text{ClO}_4(\text{H}_2\text{O})_x$  (s) (red), in comparison with the absorption spectrum of  $\text{NpO}_2^+$  in aqueous solution (left y axis, blue,  $C_{\text{Np(V)}} = 1.86 \text{ mM}$ ,  $t = 25^\circ\text{C}$ ).

previously discussed, the absence of data in the literature is probably due to either inadequate experimental conditions (e.g., low ligand/metal ratio) or failure to identify this “silent” species in the near-IR optical absorption.

The formations of both  $\text{NpO}_2(\text{DPA})^-$  and  $\text{NpO}_2(\text{DPA})_2^{3-}$  are highly exothermic ( $\Delta H = -25.2$  and  $-45.9 \text{ kJ/mol}$ ), drastically different from the 1:1 complexation of Np(V) with dicarboxylic acids without a nitrogen donor, such as malonic acid (+1.0 kJ/mol) and oxidiacetic acid (+8.7 kJ/mol).<sup>37</sup> Evidently, the energy gained in the formation of the Np–N bond significantly exceeds the energy required to desolvate the  $\text{NpO}_2^+$  cation, as well as the N atom to a much lesser extent. It is surprising that the stepwise entropy of complexation for  $\text{NpO}_2(\text{DPA})_2^{3-}$  is near zero (Table 2). We hypothesize that the formation of a highly symmetrical hexagonal  $\text{NpO}_2(\text{DPA})_2^{3-}$  could lead to a highly ordered solvent structure surrounding the complex and result in a significant loss of entropy. Additional thermodynamic data on complexes with similar coordination modes and symmetry could help test this hypothesis.

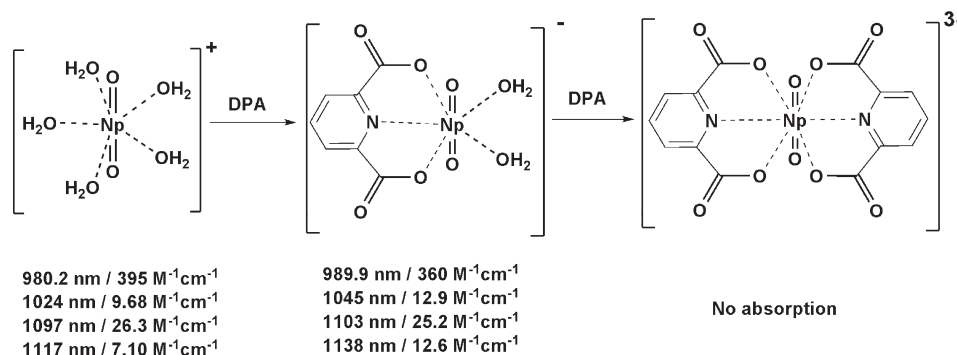
**4.2. Symmetry and Optical Absorption.** Similar to the observations in previous studies of Np(V) complexation with ODA and TMOGA,<sup>16,17</sup> the successive complexation of Np(V) with DPA and the accompanying changes

(37) Jensen, M. P.; Nash, K. L. *Radiochim. Acta* **2001**, *89*, 557.

(38) Eberle, S. H.; Wade, U. *J. Inorg. Nucl. Chem.* **1970**, *32*, 109.

(39) Smith, R. M.; Martell, A. E. *Critical Stability Constants*; Plenum Press: New York, 1989; Vol. 6.

Scheme 1



in symmetry and absorption spectra are best illustrated by Scheme 1. The free  $\text{NpO}_2^+$  cation has five  $\text{H}_2\text{O}$  molecules in the equatorial plane,<sup>40</sup> resulting in a structure without an inversion center. As a result, the  $f \rightarrow f$  transitions are allowed and the absorption bands at 980, 1024, 1097, and 1117 nm observed. For the same reason, the first complex,  $\text{NpO}_2(\text{DPA})^-$ , absorbs, but the energies are correspondingly red-shifted (989.9, 1045, 1103, and 1138 nm). However, the second complex,  $\text{NpO}_2(\text{DPA})_2^{3-}$ , is highly symmetrical with an inversion center, and the  $f \rightarrow f$  transitions are forbidden so that the  $\text{NpO}_2(\text{DPA})_2^{3-}$  complex in solution has no absorption in the near-IR region (Figure 2c) and the sharp bands typical of  $f \rightarrow f$  transitions disappear or become very weak in the diffuse reflectance spectrum of solid  $\text{Na}_3\text{NpO}_2(\text{DPA})_2(\text{H}_2\text{O})_6$  (Figure 5).

It is worth noting an interesting feature of the absorption bands of  $\text{Np(V)}$  in the near-IR region. As shown in Figure 2c and Scheme 1, all four bands of free  $\text{NpO}_2^+$  are red-shifted, and the intensities change when forming  $\text{NpO}_2(\text{DPA})^-$ . However, the magnitudes of band shifts and intensity changes are different for the four bands. In fact, two bands (980 and 1097 nm) are red-shifted by 6–10 nm and their intensities decrease by 5–10% in  $\text{NpO}_2(\text{DPA})^-$ , while the other two bands (1024 and 1117 nm) are red-shifted by 21 nm and the intensities increase by 30–80%. In brief, the intensities of the bands with smaller red shifts decrease, but the intensities of the bands with larger red shifts increase when  $\text{NpO}_2^+$  forms  $\text{NpO}_2(\text{DPA})^-$ . Future theoretical calculations on the changes of the energy levels and transition probabilities in the  $5f^2$  electronic system could provide more insight into this interesting observation.

**4.3. Implication for the Complexation of  $\text{Np(V)}$  with Dipicolinamides: Amide Group versus Carboxylate Group.** Previous studies have shown that ODA and its diamide derivative (TMOGA) form tridentate  $\text{Np(V)}$  complexes with similar structures, but the contributions of enthalpy and entropy to the stability of the complexes differ between the acid complex and the amide complex.<sup>11</sup> By analogy, the results on the complexation of  $\text{Np(V)}$

with DPA from this work have the following implications: (1) Dipicolinamides are expected to form trident complexes with  $\text{Np(V)}$  with similar structures to those in the  $\text{Np(V)}$ –DPA complexes. (2) The enthalpy of  $\text{Np(V)}$ –dipicolinamide complexation would be more exothermic and more favorable than that of  $\text{Np(V)}$ –DPA complexation, because the  $-\text{C}=\text{O}$  unit in the amide group has been shown to be less solvated and requires less desolvation energy than the  $-\text{COO}^-$  unit in the carboxylate group.<sup>11</sup> More favorable enthalpy will make dipicolinamides stronger complexants than DPA and potentially excellent extractants for  $\text{Np(V)}$ . (3) In contrast to the effect of enthalpy, the entropy of  $\text{Np(V)}$ –dipicolinamide complexation would be smaller and less favorable than that of  $\text{Np(V)}$ –DPA complexation, because fewer solvent molecules are released in the complexation with amides than carboxylates.<sup>11</sup> This means that, to strengthen the complexation of dipicolinamides with  $\text{Np(V)}$  and improve its efficiency in extracting  $\text{Np(V)}$ , enlarging the entropy effect (e.g., designing picolinamides of higher denticity) should be a plausible approach.

## 5. Conclusion

The 1:2  $\text{Np(V)}$ –DPA complex,  $\text{NpO}_2(\text{DPA})_2^{3-}$ , was identified in a solid by single-crystal X-ray diffractometry, and in solution by absorption spectroscopy for the first time. Thermodynamic parameters and structural data of  $\text{Np(V)}$ –DPA complexes from this work provide help with the development of dipicolinamide ligands as efficient extractants for separating  $\text{Np(V)}$  in advanced nuclear energy systems.

**Acknowledgment.** This research was supported by the Director, Office of Basic Energy Science, Office of Basic Energy Science of the U.S. Department of Energy (DOE) under Contract No. DE-AC02-05CH 11231 at Lawrence Berkeley National Laboratory (LBNL). The Advanced Light Source (ALS) was operated by LBNL for DOE. The authors are grateful to the anonymous reviewers whose comments have helped to significantly improve the manuscript.

**Supporting Information Available:** A crystallographic information file is provided. This material is available free of charge via the Internet at <http://pubs.acs.org>.

(40) (a) Combes, J. M.; Chisholm-Brause, C. J.; Brown, G. E.; Parks, G. A., Jr.; Conradson, S. D.; Eller, P. G. I.; Triay, R.; Hobart, D. E.; Meijer, A. *Environ. Sci. Technol.* **1992**, *26*, 376. (b) Allen, P. G.; Bucher, J. J.; Shuh, D. K.; Edelstein, N. M.; Reich, T. *Inorg. Chem.* **1997**, *36*, 4676.